

# A new comprehensive study of the 3D random-field Ising model via sampling the density of states in dominant energy subspaces

Nikolaos G. Fytas\* and Anastasios Malakis

*Department of Physics, Section of Solid State Physics,  
University of Athens, Panepistimiopolis,  
GR 15784 Zografos, Athens, Greece*

## Abstract

The three-dimensional bimodal random-field Ising model is studied via a new finite temperature numerical approach. The methods of Wang-Landau sampling and broad histogram are implemented in a unified algorithm by using the N-fold version of the Wang-Landau algorithm. The simulations are performed in dominant energy subspaces, determined by the recently developed critical minimum energy subspace technique. The random-fields are obtained from a bimodal distribution, that is we consider the discrete ( $\pm\Delta$ ) case and the model is studied on cubic lattices with sizes  $4 \leq L \leq 20$ . In order to extract information for the relevant probability distributions of the specific heat and susceptibility peaks, large samples of random-field realizations are generated. The general aspects of the model's scaling behavior are discussed and the process of averaging finite-size anomalies in random systems is re-examined under the prism of the lack of self-averaging of the specific heat and susceptibility of the model.

PACS numbers: 05.70.Jk, 64.60.Fr, 75.10.Hk, 75.50.Lk

Keywords: random-field Ising model, Wang-Landau sampling, broad histogram, self-averaging

---

\*Corresponding author: nfyas@phys.uoa.gr

## I. INTRODUCTION

The random-field Ising model (RFIM) [1] is one of the most studied glassy magnetic models [2, 3, 4]. The 3D RFIM consists of Ising spins  $S_i$  on a simple cubic lattice, governed by the Hamiltonian:

$$\mathcal{H} = -J \sum_{\langle i,j \rangle} S_i S_j - \sum_i h_i S_i \quad (1)$$

where  $J > 0$  is the interaction constant and  $h_i$  are quenched random-fields, obtained from a bimodal distribution  $P(h_i) = \frac{1}{2}\delta(h_i - \Delta) + \frac{1}{2}\delta(h_i + \Delta)$ .  $\Delta$  denotes the disorder strength, also called randomness of the model. Although nowadays it is believed that the phase transition from the ordered to the disordered phase of the model is of second-order, a complete set of critical exponents fulfilling a widely accepted set of scaling relations has not been established. In fact, there is a strong disagreement in literature concerning the overall thermal and magnetic behavior of the model [5, 6]. This may be due to a mistaken comprehension of some theoretical concepts in random systems, such as the concept of averaging that will be discussed below.

The rest of the paper is laid out as follows. In Section II we present the numerical schemes utilized for the study of the RFIM. The process of averaging finite-size anomalies in random systems and the significance and implications of the non trivial property of the lack of self-averaging of the specific heat and susceptibility of the model, are discussed in Section III. Finally, we summarize in Section IV.

## II. NUMERICAL TECHNIQUES

Numerically the RFIM has been approached using traditional [7, 8] but also more sophisticated Monte Carlo techniques [9]. However, the nature of the model demands enormous computer resources. Furthermore, in order to get a good estimate of the mean properties of the system, it is necessary to repeat the simulations for a large number of realizations of the random-fields. Here, the numerical procedure concentrates on the determination of the density of states (DOS)  $G(E)$  of the model and on the corresponding thermodynamic quantities.

For the application of the Wang-Landau (WL) algorithm [10] in a multi-range approach we follow the N-fold description of Schulz *et al.* [11]. The random walk is not allowed to

move outside of any particular subrange, and we always increment the histogram  $H(E) \rightarrow H(E) + 1$  and the DOS  $G(E) \rightarrow G(E) * f_j$  after a spin-flip trial. Here,  $f_j$  is the value of the WL modification factor  $f$  [10] at the  $j$ th iteration, in the process ( $f \rightarrow f^{1/2}$ ) of reducing its value to 1, where the detailed balance condition is satisfied. In all our simulations the control parameter takes the initial value:  $f_{j=1} = e \approx 2.71828...$ , while when starting a new iteration it is changed according to the sequence  $f_{j+1} = \sqrt{f_j}$ ,  $j = 1, 2, \dots, 20$  [10, 12]. For the histogram flatness criterion we use a flatness level of 0.05. The accumulation of numerical data for the application of the broad histogram (BH) method of Oliveira *et al.* [13] and also the updating of appropriate  $(E, M)$  histograms is carried out in the final stage of the WL process, by using the N-fold iteration  $j = 12 - 20$  [14]. The approximation of the DOS, in the last WL iteration,  $G_{WL}(E)$ , and the high-level ( $j \gg 1$ ) WL  $(E, M)$  histograms,  $H_{WL}(E, M)$ , are then used to estimate the magnetic properties in a temperature range, which is covered, by the restricted energy subspace  $(E_1, E_2)$  as:

$$\langle M^n \rangle = \frac{\sum_E \langle M^n \rangle_E G(E) e^{-\beta E}}{\sum_E G(E) e^{-\beta E}} \cong \frac{\sum_{E \in (E_1, E_2)} \langle M^n \rangle_{E, WL} G_{WL}(E) e^{-\beta E}}{\sum_{E \in (E_1, E_2)} G_{WL}(E) e^{-\beta E}} \quad (2)$$

The microcanonical averages  $\langle M^n \rangle_E$  are obtained from the  $H_{WL}(E, M)$  histograms as:

$$\begin{aligned} \langle M^n \rangle_E &\cong \langle M^n \rangle_{E, WL} \equiv \sum_M M^n \frac{H_{WL}(E, M)}{H_{WL}(E)} \\ H_{WL}(E) &= \sum_M H_{WL}(E, M) \end{aligned} \quad (3)$$

and the summation in  $M$  runs over all values generated in the restricted energy subspace  $(E_1, E_2)$  [14]. Similarly we obtain the microcanonical estimators necessary for the application of the BH method, using the well-known broad histogram equation [13]:

$$G(E) \langle N(E, E + \Delta E_n) \rangle_E = G(E + \Delta E_n) \langle N(E + \Delta E_n, E) \rangle_{E + \Delta E_n} \quad (4)$$

where  $N(E, E + \Delta E_n)$  is the number of possible spin flip moves from a microstate of energy  $E$  to a microstate with energy  $E + \Delta E_n$ , which are known during the N-fold process.

For a particular random-field realization the specific heat and its peak are easily obtained with the help of the usual statistical sums. The critical minimum energy subspace (CrMES) scheme [12, 14] uses only a small but dominant part  $(\tilde{E}_-, \tilde{E}_+)$  of the total energy space  $(E_{min}, E_{max})$  to determine the specific heat peaks. Let  $\tilde{E}$  denotes the value of energy producing the maximum term in the partition function at the pseudocritical temperature

(corresponding to the specific heat peak) and  $S(E) = \ln G(E)$  the microcanonical entropy. Then the CrMES approximation is defined by the following equations:

$$C_L(\tilde{E}_-, \tilde{E}_+) = N^{-1}T^{-2} \left\{ \tilde{Z}^{-1} \sum_{\tilde{E}_-}^{\tilde{E}_+} E^2 \exp[\tilde{\Phi}(E)] - \left( \tilde{Z}^{-1} \sum_{\tilde{E}_-}^{\tilde{E}_+} E \exp[\tilde{\Phi}(E)] \right)^2 \right\} \quad (5)$$

$$\tilde{\Phi}(E) = [S(E) - \beta E] - [S(\tilde{E}) - \beta \tilde{E}], \quad \tilde{Z} = \sum_{\tilde{E}_-}^{\tilde{E}_+} \exp[\tilde{\Phi}(E)] \quad (6)$$

where  $(\tilde{E}_-, \tilde{E}_+)$  is the minimum dominant subrange, satisfying the following accuracy criterion:

$$\left| \frac{C_L(\tilde{E}_-, \tilde{E}_+)}{C_L(E_{min}, E_{max})} - 1 \right| \leq r \quad (7)$$

with  $r = 10^{-6}$ . Note that, the above accuracy is extremely demanding compared to the statistical errors produced by the DOS method (i.e. the WL method) and to the large sample-to-sample fluctuations of the RFIM that will be discussed below in Section III.

Using an ensemble of macroscopic samples of size  $L$  corresponding to different random-field realizations we have applied the described scheme in a broad energy(magnetization) space (total CrME(M)S of the ensemble) that covers the overlap of the dominant energy(magnetization) subspaces for all realizations of the ensemble. This practice has the advantage that the approximation of the specific heat and susceptibility for a particular random-field is accurate in a wide temperature range, including its pseudocritical temperature. Despite the strong fluctuations of the energy value corresponding to the maximum term of the partition function  $Z$ , the union of the CrME(M)S for large samples of random-fields is, in any case, a quite small subspace.

### III. AVERAGING FINITE-SIZE ANOMALIES. LACK OF SELF-AVERAGING

For a disordered system one has to perform two distinct kinds of averaging. Firstly, for each random-field realization the usual thermal average has to be carried out and secondly one must average over the distribution of the random parameters. The latter makes it clear that large ensembles of random-fields must be generated in order to estimate properly the mean properties of the system. Following the methods described above in Section II the

thermal average for the specific heat is given by Eq. (5), while the susceptibility  $\chi$  reads as:

$$\chi = \frac{N}{T} \{ \langle M^2 \rangle - \langle M \rangle^2 \} \quad (8)$$

with  $N = L^3$ . Let  $C_m(T)$  and  $\chi_m(T)$  denote the specific heat and susceptibility of a particular random-field realization  $m$  in an ensemble of  $M$  realizations ( $m = 1, 2, \dots, M$ ). The corresponding pseudocritical temperatures  $T_L^*(C_m(T))$  and  $T_L^*(\chi_m(T))$  depend on the particular realization of the random-field and for large values of the randomness  $\Delta$ , they are strongly fluctuating quantities. The locations of the specific heat and susceptibility peaks may be then denoted by  $(C_m^*, T_{L,C;m}^*)$  and  $(\chi_m^*, T_{L,\chi;m}^*)$ , respectively.

In previous studies [7, 8], the averaging process over a large number of random-fields has been carried out on the averaged curve of the specific heat or susceptibility, without first raising the question of whether this averaged curve is the proper statistical representative of the system. Specifically, the following sample averages have been considered for the specific heat and susceptibility [7, 8]:

$$[C]_{av} = \frac{1}{M} \sum_{m=1}^M C_m(T); \quad [\chi]_{av} = \frac{1}{M} \sum_{m=1}^M \chi_m(T) \quad (9)$$

The finite-size scaling behavior of the peak of these averaged curves was then studied by assuming that the maxima  $[C]_{av}^* = ([C]_{av})^*$  and  $[\chi]_{av}^* = ([\chi]_{av})^*$  obey power laws (for details see Refs. [7, 8]). Note that, these averaged curves ( $[C]_{av}$  and  $[\chi]_{av}$ ) are very sensitive to the property of self-averaging due to the fact that the corresponding thermodynamic quantities are characterized by broad distributions in the thermodynamic limit.

In this work, in addition to the above averaging expressions, we study the sample-averages of the individual specific heat and susceptibility maxima, defined by:

$$[C_m^*]_{av} = \frac{1}{M} \sum_{m=1}^M C_m^*; \quad [\chi_m^*]_{av} = \frac{1}{M} \sum_{m=1}^M \chi_m^* \quad (10)$$

These mean values, together with the corresponding peaks of the averaged curves of Eq. (9), are shown in Figs. 1,2. In our simulations we used an ensemble of  $M = 1000$  random-field realizations for  $L \leq 12$  and  $M = 500$  for  $L = 14 - 20$ . To quantify the sample-to-sample fluctuations of the specific heat (susceptibility) peaks we define the standard deviation of  $C_m^*$  ( $\chi_m^*$ ), over a sample of  $M$  random-field realizations as  $\sigma(C_m^*)$  ( $\sigma(\chi_m^*)$ ). This important parameter will be illustrated in our figures as error bars, but should not be in any case confused with the existing statistical errors.

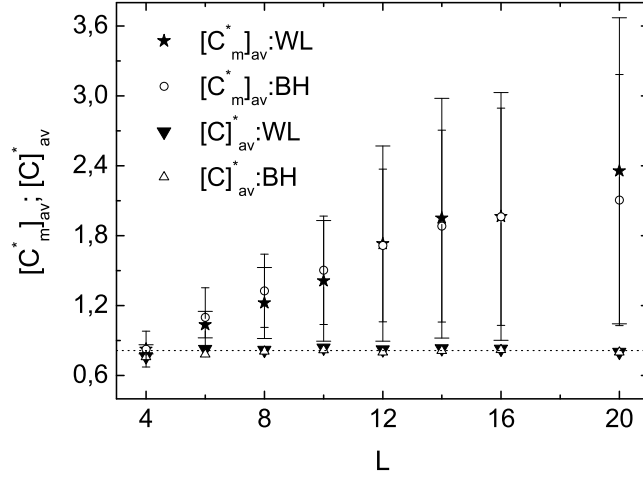


FIG. 1: Finite-size behavior of the averages  $[C_m^*]_{av}$  and  $[C]_{av}^*$  for the case  $\Delta = 2$ , for both the WL and BH methods used. The error bars represent the sample-to-sample fluctuations (see text). The behavior of  $[C]_{av}^*$  appears as a random fluctuation around the value 0.815, as shown by the dotted line.

Fig. 1 illustrates the finite-size behavior of the peaks of the average  $[C_m^*]_{av}$  and that of the averaged curve  $[C]_{av}^*$ , defined above for the case  $\Delta = 2$  for the two methods employed, i.e. the WL and BH methods. As discussed above, the error bars quantify the large sample-to-sample fluctuations of the specific heat peaks for the two methods employed (note that the error bars with the larger cap-width always refer to the WL method). From Fig. 1 it is apparent that, while the sample mean averages  $[C_m^*]_{av}$  admits of finite-size scaling, the behavior of  $[C]_{av}^*$  appears as a random fluctuation around the value  $[C]_{av}^* \approx 0.815$ , as shown by the dotted line in this figure. In analogy with Fig. 1, Fig. 2 shows the corresponding susceptibility quantities, also for the case  $\Delta = 2$ . Again, the sample-to-sample fluctuations are very large and the behavior of  $[\chi]_{av}^*$  is clearly distinct from that of  $[\chi_m^*]_{av}$ . Inspecting Figs. 1,2 on a comparative basis we observe that the deviations between the WL and BH methods are more pronounced in the thermal case (Fig. 1) and their difference is noticeable for  $L = 20$ . This difference represents the order of the statistical errors of our scheme. Although these errors are still small compared to the sample-to-sample fluctuations, they raise doubts whether the total number of WL iterations ( $j_{final} = 20$ ) is sufficient for the

study of large lattice sizes.

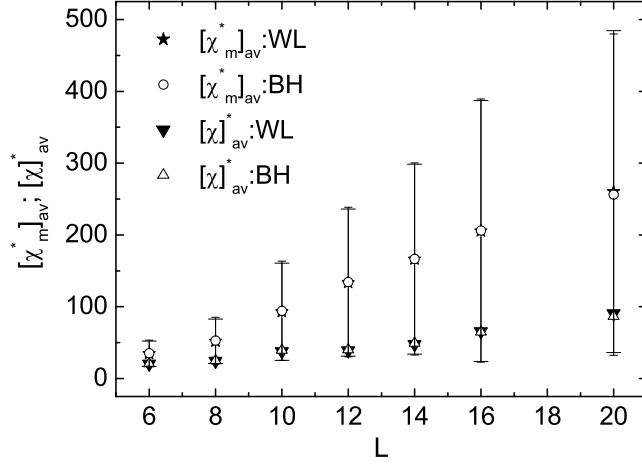


FIG. 2: Finite-size behavior of the averages  $[\chi_m^*]_{av}$  and  $[\chi]^*_{av}$  for the WL and BH methods, also for the case  $\Delta = 2$ .

From the discussion above, it is clear that when studying random systems the only meaningful objects for investigating the finite-size scaling behavior are the distributions of various properties in ensembles of several realizations of the randomness. Hence, it is important to be able to ascertain to what extent are the results obtained from an ensemble of random realizations representative of the general class to which the system belongs. The answer hinges on the important issue of self-averaging. If a quantity is not self-averaging, we talk about lack of self-averaging and the process of increasing  $L$  does not improve the statistics. In other words, the sample-to-sample fluctuations remain large. The problem of self-averaging in the 3D RFIM has been a matter of investigation over the last years [15]. A common measure characterizing the self-averaging property of a system based on the theory of finite-size scaling has been discussed by Binder [16] and has been used for the study of some random systems [17, 18]. This measure inspects the behavior of a normalized square width quantity, defined as:

$$R_Q = \frac{V_Q}{[Q]^2} \quad (11)$$

where  $V_Q = [Q^2] - [Q]^2$  is the sample-to-sample variance of the average  $[Q]$ . Here,  $Q$  is used in respect of the specific heat  $C$  and the susceptibility  $\chi$ . According to the literature [16, 17, 18]

when the ratio  $R_Q$  tends to a constant, the system is said to be non self-averaging and the corresponding distribution (say  $P(Q)$ ) does not become sharp in the thermodynamic limit.

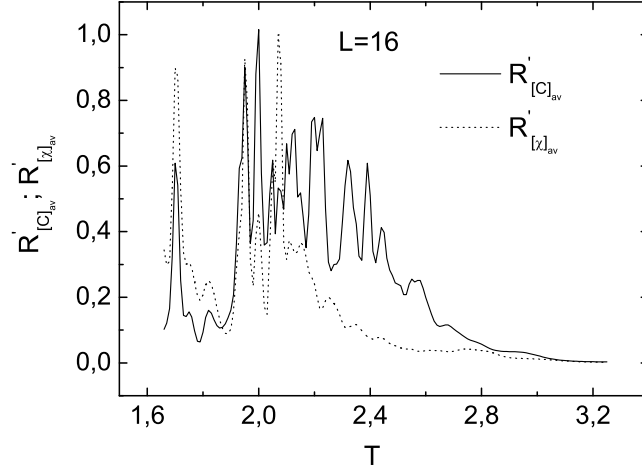


FIG. 3: Temperature variation of the ratio  $R'_{[Q]_{av}}$  defined in the text, for both the specific heat and susceptibility.

Using our notation we may define the ratio  $R_Q$  for the specific heat and susceptibility in two explicit forms, one for the case of the averaged curve  $[Q]_{av}$ :

$$R_{[C]_{av}} = \frac{V_{[C]_{av}}}{([C]_{av})^2}, \quad R_{[\chi]_{av}} = \frac{V_{[\chi]_{av}}}{([\chi]_{av})^2} \quad (12)$$

and one for the case of the average  $[Q_m^*]_{av}$ :

$$R_{[C_m^*]_{av}} = \frac{V_{[C_m^*]_{av}}}{([C_m^*]_{av})^2} = \left( \frac{\sigma(C_m^*)}{[C_m^*]_{av}} \right)^2, \quad R_{[\chi_m^*]_{av}} = \frac{V_{[\chi_m^*]_{av}}}{([\chi_m^*]_{av})^2} = \left( \frac{\sigma(\chi_m^*)}{[\chi_m^*]_{av}} \right)^2 \quad (13)$$

In Fig. 3 we present the behavior of the ratio  $R'_{[Q]_{av}} = R_{[Q]_{av}}/R_{[Q]_{av}}^*$ , where  $R_{[Q]_{av}}^* = \max\{R_{[Q]_{av}}\}$  as a function of the temperature  $T$ , for  $L = 16$  and  $\Delta = 2$ . The solid line corresponds to the specific heat ( $R'_{[C]_{av}}$ ) while the dotted line to the susceptibility ( $R'_{[\chi]_{av}}$ ). In this figure only the results of the WL method are presented, since our intention was to identify the temperature variation of the non self-averaging property of the averaged specific heat and susceptibility defined in Eq. (9). Indeed, from Fig. 3 we observe that for temperatures close to the critical, the ratio  $R_{[Q]_{av}}$  is maximized indicating strongly non self-averaging behavior for both quantities. In Fig. 4 we consider the behavior of the ratio  $R_{[Q_m^*]_{av}}$  of the



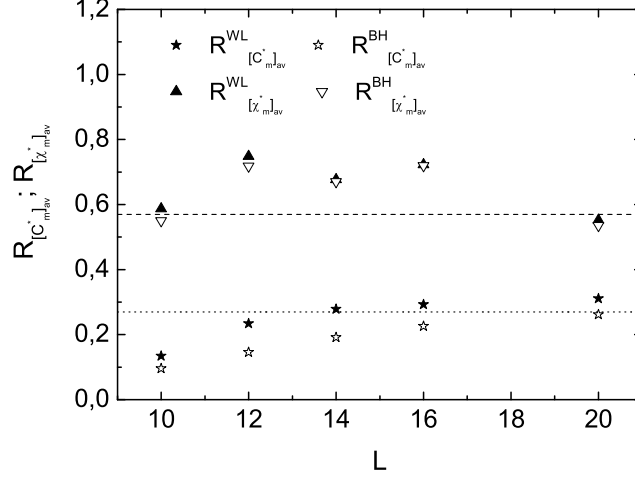


FIG. 4: Illustration of the ratio  $R_{[Q_m^*]_{av}}$  of the specific heat and susceptibility, for both the WL and BH methods, for randomness  $\Delta = 2$ . Clear saturation to a limiting non-zero constant value:  $R_{[C_m^*]_{av}} \rightarrow 0.28$  and  $R_{[\chi_m^*]_{av}} \rightarrow 0.57$ .

specific heat ( $R_{[C_m^*]_{av}}$ ) and susceptibility ( $R_{[\chi_m^*]_{av}}$ ) as a function of the linear size  $L$ , for both the WL and BH methods. Both ratios seem to tend to a constant non-zero value, namely  $R_{[C_m^*]_{av}} \rightarrow 0.28$  and  $R_{[\chi_m^*]_{av}} \rightarrow 0.57$ , confirming the above mentioned lack of self-averaging of the specific heat and susceptibility of the model.

#### IV. SUMMARY AND OUTLOOK

The numerical strategy applied in this paper enabled us to perform extensive finite-temperature simulations and extract valuable information for the generic behavior of the RFIM. It was shown that the various definitions of the apparent finite-size anomalies may not be equivalent. Our analysis revealed that the behavior of the mean  $[Q_m^*]_{av}$  is clearly distinct from that of  $[Q]_{av}^*$  and that this is directly connected to the lack of self-averaging of the model. More work needs to be done towards this direction, so that the subtle matter of self-averaging in the RFIM is fully clarified and understood. One of our future plans, is the verification of the above results by studying the model for larger lattice sizes and various randomness values. In any case, the present study puts forward some new ideas and an efficient unified implementation of the DOS methods, suitable for the study of random

systems.

## Acknowledgments

This research was supported by NKUA/SARG under Grant No. 70/4/4071.

---

- [1] Y. Imry and S.-K. Ma, Phys. Rev. Lett. **35**, 1399 (1975).
- [2] J. Z. Imbrie, Phys. Rev. Lett. **53**, 1747 (1984); Commun. Math. Phys. **98**, 145 (1985).
- [3] J. Bricmont and A. Kupiainen, Phys. Rev. Lett. **59**, 1829 (1987).
- [4] See, e.g the articles by D. P. Belanger and T. Nattermann in *Spin Glasses and Random Fields* (World Scientific, Singapore, 1998).
- [5] A. A. Middleton and D. S. Fisher, Phys. Rev. B **65**, 134411 (2002).
- [6] A. K. Hartmann and A. P. Young, Phys. Rev. B **64**, 214419 (2001).
- [7] H. Rieger and A. P. Young, J. Phys. A **26**, 5279 (1993).
- [8] H. Rieger, Phys. Rev. B **52**, 6659 (1995).
- [9] M. E. J. Newman and G. T. Barkema, Phys. Rev. E **53**, 393 (1996).
- [10] F. Wang and D. P. Landau, Phys. Rev. Lett. **86**, 2050 (2001); Phys. Rev. E **64**, 056101 (2001).
- [11] B. J. Schulz, K. Binder, M. Muller, and D. P. Landau, Phys. Rev. E **67**, 067102 (2003).
- [12] A. Malakis, A. S. Peratzakis, and N. G. Fytas, Phys. Rev. E **70**, 066128 (2004).
- [13] P. M. C. de Oliveira, T. J. P. Penna, and H. J. Herrmann, J. Braz. Phys. **26**, 677 (1996).
- [14] A. Malakis *et al.*, Phys. Rev. E **72**, 066120 (2005).
- [15] G. Parisi and N. Surlas, Phys. Rev. Lett. **89**, 257204 (2002).
- [16] K. Binder and D. W. Heermann, *Monte Carlo Simulations in Statistical Physics* (Springer-Verlag, Berlin, 1988).
- [17] S. Wiseman and E. Domany, Phys. Rev. E **52**, 3469 (1995); Phys. Rev. Lett. **81**, 22 (1998).
- [18] A. Aharony and A. B. Harris, Phys. Rev. Lett. **77**, 3700 (1996).